

Development of a Polymer-carbon Nanotubes based Economic Solar Collector

Sung in Kim¹, John Kissick¹, Stephen Spence¹ and Christine Boyle²

¹ School of Mechanical & Aerospace Engineering, Queen's University Belfast, Belfast (UK)

² Lawell Asphalt Company, Belfast (UK) (christine@asphaltroofing.com)

Abstract

A low cost solar collector was developed by using polymeric components as opposed to metal and glass components of traditional solar collectors. In order to utilize polymers for the absorber of the solar collector, Carbon Nanotubes (CNT) has been added as a filler to improve the thermal conductivity and the solar absorptivity of polymers. The solar collector was designed as a multi-layer construction with considering the economic manufacturing. Through the mathematical heat transfer analysis, the performance and characteristics of the designed solar collector have been estimated. Furthermore, the prototypes of the proposed system were built and tested at a state-of-the-art solar simulator facility to evaluate the actual performance of the developed solar collector. The cost-effective polymer-CNT solar collector, which achieved efficiency as much as that of a conventional glazed flat plate solar panel, has been successfully developed.

Key-words: Renewable energy, Flat plate, Heat transfer analysis, Efficiency, Cost-effective, Prototype

1. Introduction

Renewable energy has been being firstly considered for a sustainable energy future. The exploration for a sustainable way to use energy has been increasingly required due to fossil fuel price increase, climate change and the associated adverse environmental impact. Solar energy can play a significant role to substitute non-renewable energy sources. Solar water heating systems (SWHS), which are one type of valuable and feasible solar energy devices, are very common systems, extensively used in many countries. SWHS offer an opportunity to reduce carbon dioxide (CO₂) emissions from homes and buildings and contribute to the UK Government's target of generating 15% of the UK's energy supplies from renewable sources by 2020 (DECC, 2012)

Conventional flat plate solar collectors have been using a metal absorber plate and glass cover to transform solar energy into heat. In this collector, the incident solar energy is converted into heat and transmitted to a transfer medium, such as water. In the design of solar collector components, the transparent covers and the radiation absorber should have more attention. Glass is quite a common choice as a cover for solar thermal devices since it absorbs almost the infrared radiation (IR) re-emitted by the absorber plate. The use of a glass cover has two major disadvantages: its high installation cost and its fragility both during transportation and in service. Typically, the absorber of metals, which have large heat conductivities, is painted with black, solar selective paint to improve collector efficiency, and then it causes an extra cost. However, the total weight and cost of the traditional solar collector is significant due to the high densities and values of metals and glass. Therefore, the use of plastic polymers has been recommended because of their low weight and good resistance against shocks (Dorfling et al., 2010; Tsilingiris, 1999; Wijesundera and Iqbal, 1991).

According to the demand of cost-effective renewable energy sources, polymers have been investigated as an alternative material for the absorbers and covers. The significant potential of polymer materials for the design and mass fabrication of low cost solar collectors has been shown (Dorfling et al., 2010; Tsilingiris,

1999; Avraham et al., 2002; Abtahi, 1993). The extensive use of recyclable polymer solar collectors in assembly through on or a few extrusions allows not only a significant cost reduction of the solar water heating systems, but can also minimize the associated installation plumbing.

An economic solar collector was developed by using polymeric components of the transparent cover and the solar radiation absorber. The solar collector was designed as a multi-layer construction with considering the economic manufacturing and selecting an effective material. Through the mathematical heat transfer analysis, the performance and characteristics of the solar collector have been estimated. Furthermore, the prototypes of the proposed system were built and tested at a state-of-the-art solar simulator facility to evaluate the actual performance of the developed solar collector. Finally the design of production model was introduced.

2. Collector design and construction of prototypes

The major disadvantage of using polymer materials in collector absorber is their low thermal conductivity as compared to metal absorbers. In order to increase of thermal conductance, heat transfer paths between the absorbing surface and the heat transfer fluid have been maintained as short as possible. Therefore, the current widespread design trend of polymer absorbers is to maintain maximum contact between the absorbing surface and the heat transfer fluid using as thin layer of polymer as possible for the absorber plates (Tsilingiris, 1999).

The addition of fillers is a way to improve the low thermal conductivity of polymers (in the range of 0.1 to 0.5 W/m·K). However, the addition of large amounts of filler material changes the mechanical properties of the polymer, possibly making it unsuitable for the application. Carbon Nanotubes (CNT) have very high thermal conductivity (2000 – 6000 W/m·K) and a super aspect ratio so allowing good percolation at low concentrations (Tripanagnostopoulos et al., 2000; Mark, 2007). The samples of difference polymers, such as polycarbonate, polypropylene, polyvinyl chloride and polyethylene, with several configurations (0%, 2% and 4% CNT concentration by mass) have been produced. 2% CNT impregnated polycarbonate was selected as a material of the absorber of the solar collector, since it would have significantly improved thermal conductivity and a higher absorbance of solar radiation, while still retaining adequate mechanical properties based on the results of the radiation absorption, tensile and impact tests.

The solar collector was designed as a multi-layer structure consisting of three main polymer layers; (1) An optically transparent layer of plastic glazing above an air gap, (2) A layer of radiation absorbing polymer+CNT separating the air gap above from the water below, (3) A layer of polymer+CNT below the water, with polyurethane foam underneath. In order to absorb the rest of solar energy, which would still reach the lower surface of the water channel, and increase the total heat gain of the collector, another PC+CNT layer has been used for the lower layer of the water channel on top of insulation foam.

A good dispersion of the CNT into the polymer can be achieved by the use of a master batch of CNT impregnated polymer. Whereas the virgin polycarbonate sheet was transparent in appearance, the 2% CNT impregnated polycarbonate was a solid black color and completely opaque. The first prototype solar collector was constructed as a sample with dimensions of 500 × 500 mm (shown in Fig. 1a). Thermocouples were placed at several points on the surface of the absorber to measure the temperature distribution.



Fig. 1: The prototypes of the proposed PC+CNT solar collector: the first (a) and the second (b)

The detrimental performance effects in the first prototype test have been well observed and analyzed. Thereafter the improved second prototype has been constructed (Fig. 1b); with the aim of reducing the edge effect, the size of the second collector was increased to 1500 × 500 mm. The smooth reflective finish of the CNT impregnated polycarbonate sheet was abraded to reduce the reflectivity on its upper surface. Trapped air had been identified as an issue in the first test, with a potential negative impact on the performance. The mounting for the solar collector was redesigned to include a fixed inclination of 0.8 degrees. The inclination of the collector would encourage any air bubbles in the circulating fluid to accumulate in the uppermost manifold and prevent air pockets from gathering underneath the solar absorbing panel. The manifolds were adapted to incorporate automatic air eliminator vents that would allow any accumulating air from the circulating fluid to be vented out. Finally, the collector was encased in a wooden frame to ensure protection for the prototype and provide adequate structural rigidity to prevent flexing during transportation and installation.

3. Heat Transfer analysis

3.1. Heat transfer modeling

This section describes a mathematical heat transfer model that estimates the effect of key design parameters on the performance of the proposed solar collector. A steady state, one-dimensional heat transfer that solves the coupled radiative and convective energy balances at the solar absorbing layers in the solar collector was considered. The schematic diagram of the heat transfer in the solar collector was shown in Fig. 2. In the heat transfer analysis, uniform constant temperature of each layer was assumed. For the air between layer 1 and 2 in Fig. 2, the constant properties of ideal gas air at the mean temperature of these two layers were used. The surrounding temperature (T_{surr}) for the radiation and the ambient temperature (T_a) for the convection were assumed to be identical due to the test environment where the indoor temperature was not varied much. By ignoring the wind chill effect, the top surface temperature of the solar collector was assumed to be same to the ambient temperature ($T_1 = T_a$).

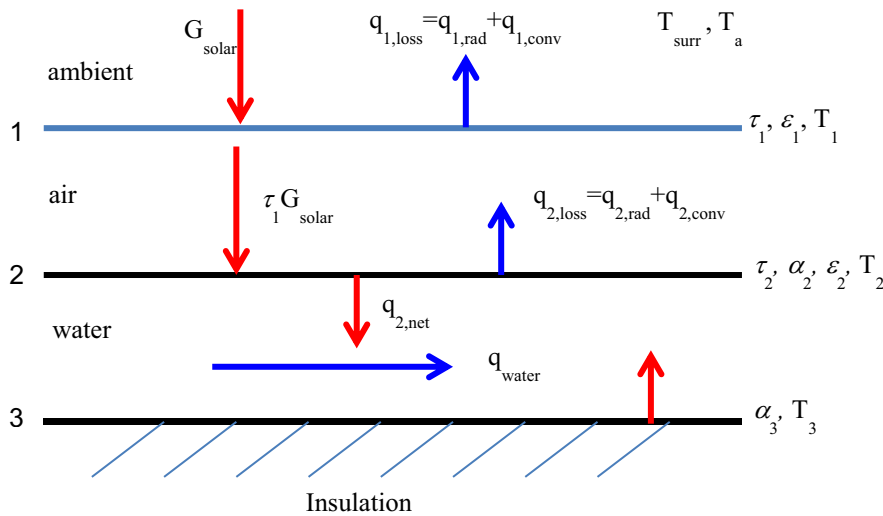


Fig. 2: The net heat transfer in the solar collector

The amounts of the absorbed heat in the second and third layers (upper and lower boundary of the heat transfer fluid, water) were determined by the optical properties of the material.

$$q_{2,absor} = \alpha_2 \tau_1 G_{solar} \quad \text{and} \quad q_{3,absor} = \alpha_3 \tau_2 \tau_1 G_{solar} \quad (\text{eq. 1})$$

where τ_1 and τ_2 were the transmissivities of the first (PC) layer and the second (PC+CNT) layer, α_2 and α_3 were the absorptivities of the second and third (PC+CNT) layers (here, $\alpha_2 = \alpha_3$ because of the same material) and G_{solar} was a given solar radiation intensity. Therefore, the maximum absorbable heat ($q_{2,absor} + q_{3,absor}$) in the solar collector was determined by only the optical properties of the absorber material. In order to gain more solar heat in the collector, higher absorptivity of the absorbing layer was required.

There was heat loss from the absorbing layer due to the temperature difference between T_1 and T_2 . The heat

loss from the absorber was represented by the two mechanisms of radiation and natural convection. The heat loss by radiation was calculated by Stefan's law which was comprised of the temperatures and emissivities of two parallel plates.

$$q_{2,rad} = \frac{\sigma(T_2^4 - T_1^4)}{\frac{1}{\varepsilon_2} + \frac{1}{\varepsilon_1} - 1} \quad (\text{eq. 2})$$

The second heat loss was caused by the natural convection due to the temperature difference between the two layers of the air gap. It was determined by the thermodynamic properties of the air (k_{air} , ν_{air} , Pr) and the geometric parameter, the air gap height, H_1 .

$$q_{2,conv} = k_{air} Nu \frac{T_2 - T_1}{H_1} \quad (\text{eq. 3})$$

$$\text{where, } Nu = 1 + 1.44 \left[1 - \frac{1708}{Ra} \right]^+ + \left[\frac{Ra^{1/3}}{18} - 1 \right]^+, \quad Ra = \frac{g\beta(T_2 - T_1)H_1^3}{\nu_{air}^2} Pr$$

The net heat gain at the second layer (layer 2 in Fig. 2) was able to be obtained by the heat balance:

$$q_{2,net} = q_{2,absor} - q_{2,rad} - q_{2,conv} \quad (\text{eq. 4})$$

$$q_{total} = q_{2,net} + q_{3,absor} = q_{2,absor} - q_{2,rad} - q_{2,conv} + q_{3,absor} = f(T_1, T_2, H_1, \text{properties}) = f(T_2) \quad (\text{eq. 5})$$

Finally, the total net heat gain of the solar collector was the sum of the net heat gain of layer 2 and the absorbed heat of layer 3. As shown in above formulas, this total net heat gain was determined by the temperatures of the layers, thermodynamic and optical properties of the air and materials, and the geometric dimension. When the top layer temperature ($T_1 = T_a$) and the dimension (H_1) were given and the properties were assumed (air as an ideal gas and the material properties as given in Table 1), the total heat gain was determined by the temperature (T_2) of the second layer (upper PC+CNT layer) only. For given dimensions and properties, the total heat gain of the solar collector was ideally maximized when the temperature of the absorbing layer (T_2) was the same as the top layer temperature (T_1); no heat loss from layer 2 to layer 1, no heat remained at the absorbing layer, and therefore all the absorbed heat was transferred to the water. When the total absorbed heat was transferred to the water, the water temperature was increased through the solar collector ($T_{out} > T_{in}$). The outlet water temperature could be calculated by the energy conservation.

$$q_{total} = \dot{m}c_p(T_{out} - T_{in})/A_s = g(T_{out}) \quad (\text{eq. 6})$$

$$\begin{aligned} \therefore q_{total} = q_{2,net} + q_{3,absor} &= \dot{m}c_p(T_{out} - T_{in})/A_s \\ \Rightarrow f(T_2) &= g(T_{out}) \end{aligned} \quad (\text{eq. 7})$$

However, once the heat balance equation was concluded, two unknown temperatures (T_2 and T_{out}) and the fourth power of temperature (T_2^4) in radiation made it difficult to solve directly. The temperatures of the absorbing layer (T_2) and the water outlet (T_{out}) were calculated iteratively. The iterative computation procedure was depicted in the diagram in Fig. 3. For a given water inlet temperature (T_{in}), the water outlet temperature (T_{out}) was initially estimated and then the total heat transfer rate (q_{total}) was calculated from the water temperature rise. The temperature of the absorbing layer (T_2) was determined to satisfy the heat balance; the total absorbed heat, $f(T_2)$, should be equal to the transferred heat, $g(T_{out})$, under the restrictive condition of ($T_2 > T_{out}$). If the transferred heat, $g(T_{out})$, was greater than the absorbed heat, $f(T_2)$, then the water outlet temperature (T_{out}) was reduced and T_2 was determined to meet the heat balance. Iteratively T_2 was calculated with decreasing T_{out} until satisfying $f(T_2) = g(T_{out})$ and $T_2 > T_{out}$.

In order to calculate the heat transfer rate in the solar collector, the base optical properties of the proposed material, PC+CNT, were assumed as shown in Table 1, based on the typical properties of the polycarbonate and the estimation from the first prototype measurement. Heat transfer analysis was firstly performed with the assumed base properties. The given solar intensity was assumed as 835 W/m^2 in the heat transfer analysis.

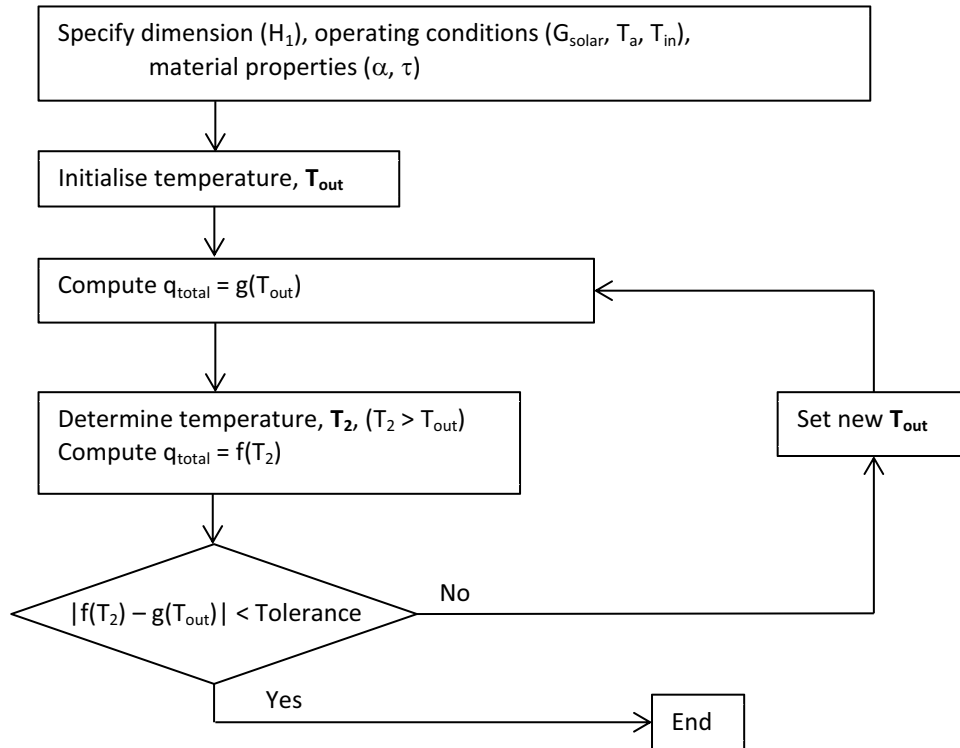


Fig. 3: The flow chart for nonlinear iterative calculation

Tab. 1: The assumptions of the optical properties of the materials of the solar collector

	Optical properties	Base values	Higher
PC glazing layer	Solar transmittance, τ_1	0.85	0.85
	Infrared emissivity, ε_1	0.5	0.5
PC+CNT upper layer	Solar absorbance, α_2	0.4	0.56
	Solar transmittance, τ_2	0.4	0.4
PC+CNT lower layer	Infrared emissivity, ε_2	0.5	0.5
	Solar absorbance, α_3	0.4	0.56

Tab. 2: Estimated base temperatures and efficiency of the CNT collector

T_a (°C)	T_{in} (°C)	T_{out} (°C)	q_{total} (W/m ²) to water	T_2 (°C)	Efficiency
20	20	24.2	373	25.4	0.447
20	25	29.0	355	29.2	0.425
20	30	33.7	328	34.8	0.393
20	35	38.4	302	39.4	0.361

(for 0.5m × 0.5m panel with the base property value, $\alpha_2 = 0.4$, in Table 1)

Tab. 3: Estimated higher temperatures and efficiency of the CNT collector

T_a (°C)	T_{in} (°C)	T_{out} (°C)	q_{total} (W/m ²) to water	T_2 (°C)	Efficiency
20	20	25.9	524	27.1	0.627
20	25	30.7	506	30.9	0.606
20	30	35.4	479	36.4	0.574
20	35	40.1	453	40.3	0.542

(for 0.5m × 0.5m panel with the higher property value, $\alpha_2 = 0.56$, in Table 1)

3.2. Estimation of the relation between absorptivity and efficiency of the solar collector

The most important points in the design of solar collector should be the efficiency of the collector and the available water outlet temperature. Using the heat transfer analysis, the available water outlet temperature of the solar collector was estimated. For the given dimensions used in the first prototype, the base properties given in Table 1 and the operating conditions of $T_a = T_{in} = 20\text{ }^\circ\text{C}$, the achievable water outlet temperature and efficiency of the solar collector were calculated and presented in Table 2. The maximum water temperature rise and efficiency were $4.2\text{ }^\circ\text{C}$ and 0.447, respectively. The estimated efficiencies were compared with the first prototype measurement and the reference of a conventional glazed flat plate solar collector with moderately selective black paint absorber in Fig. 4. The maximum efficiency with the base properties (HT 1 in Fig. 4) was much lower than the reference value. In order to achieve a comparable efficiency with the reference value, a higher solar absorptivity of the material was required. To achieve efficiency as high as the reference, the required solar absorptivity of the material, PC+CNT, was estimated. The required higher properties are also provided in Table 1. The higher water outlet temperature and efficiency achieved with the higher absorptivity value of $\alpha_2 = 0.56$ under the same dimensions and operating conditions were estimated and shown in Table 3. The maximum efficiency was around 0.63 with $\alpha_2 = 0.56$. The higher efficiency (HT 2 in Fig. 4) was also compared with the reference. Nevertheless the available water outlet temperature was still relatively low, because the total heat gain is small due to the small size of the panel.

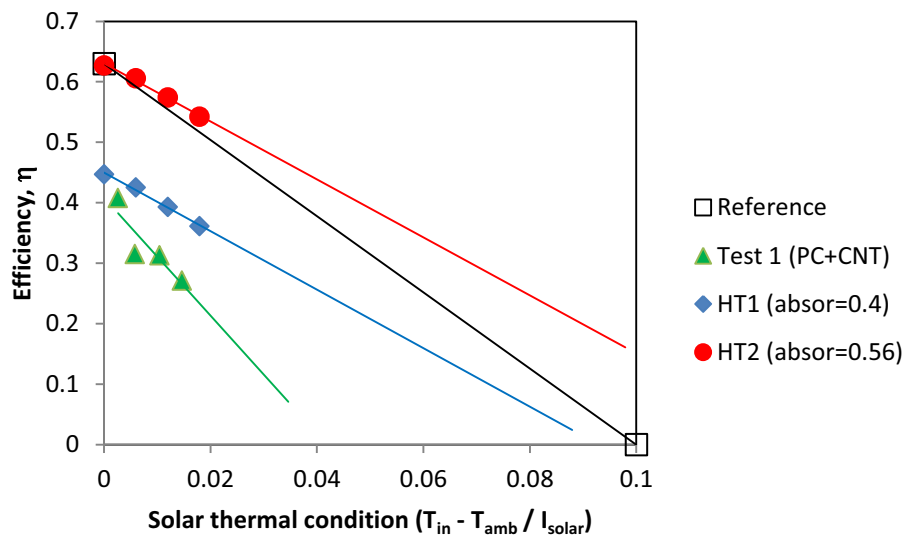


Fig. 4: The efficiency of the solar collector with different absorptivities (0.5×0.5 panel)

Tab. 4: Estimated temperatures and efficiency of the CNT collector with a larger size

T_a ($^\circ\text{C}$)	T_{in} ($^\circ\text{C}$)	T_{out} ($^\circ\text{C}$)	q_{total} (W/m^2) to water	T_2 ($^\circ\text{C}$)	Efficiency
20	20	36.2	479	36.4	0.574
20	25	40.3	453	40.3	0.542
20	30	44.1	417	44.4	0.499
20	35	48.0	384	48.2	0.461

(for $0.5\text{m} \times 1.5\text{m}$ panel with the higher property value, $\alpha_2 = 0.56$, in Table 1)

3.3. Effect of the size of the solar panel

For the given values of the material properties and the collector dimensions, the maximum achievable outlet temperatures of the water were estimated. As a result, the temperature of the water outlet was limited by the total heat gain which was depending on the optical properties of the material as well as the size of the solar collector. In order to increase the available water temperature of the solar collector under the fixed material properties, the size of the collector needed to be increased. In order to see the effect of the panel size, the outlet temperature of the water was calculated for a solar panel that was three times longer than the first prototype. The predicted results are provided in Table 4.

The maximum temperature increment was around 16 °C. As a result, the hot water over 60 °C could be achieved through the sequential connection of three solar collectors. The effect of the panel size on the efficiency of the solar collector was shown in Fig. 5. The efficiency of the larger panel (HT3 in Fig. 5) was lower than that of the smaller panel, which was attributed to the increased average temperatures of the water and absorbing layer resulting in larger heat losses.

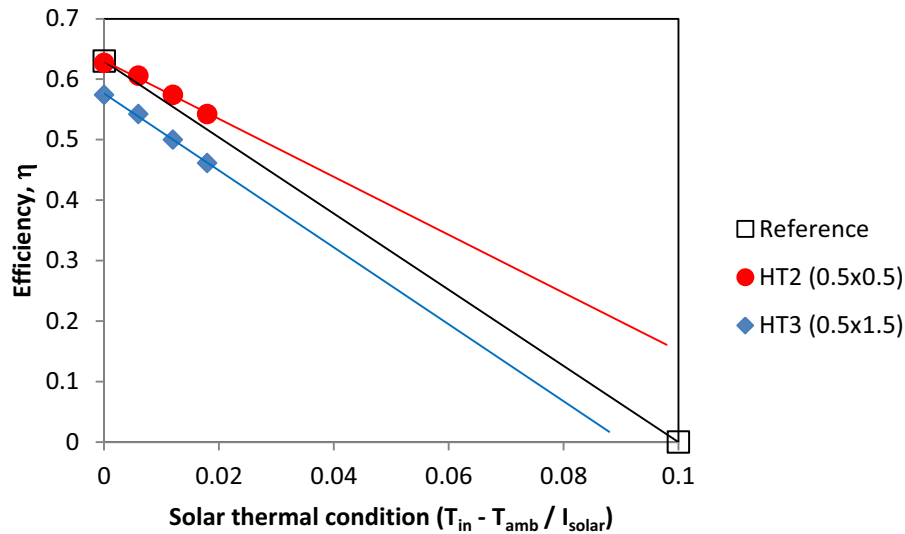


Fig. 5: The efficiencies of the solar collector with different sizes ($\alpha_2 = 0.56$)

4. Tests results and analysis

The prototype solar collectors were tested at University of Ulster using a state of the art solar rig. The testing at a solar simulator facility was conducted under the specified constant solar flux and water flow rate. The initial water temperature was set at 20 °C and increased by 5 °C intervals once steady state conditions were attained. The temperatures of ambient, water in and out, and the several points on the absorber surface were recorded.

4.1. Effect of the inclusion of Carbon Nanotubes (CNT)

In the first test, two prototype solar collector panels; one of only standard polycarbonate sheeting with no CNT included and the other of CNT included in the absorbing layers, were simultaneously tested to evaluate the performance improvement of the solar collector by the addition of the CNT. For the PC+CNT collector, the water temperature increase between inlet and outlet was obvious, whereas the PC collector showed heat loss rather than heat gain through the collector as the water inlet temperature increased. During the test the accumulation of air within the PC panel was observed, the inconsistent temperature distribution was attributed to the dispersed entrapped air which resulted in uneven heat transfer to the water flow over the absorber layer of the PC collector. However, for the PC+CNT collector the temperature distributions showed a consistent and reasonable trend; lower surface temperature around the water inlet region and higher surface temperature near the water outlet area. Finally, the efficiency of the PC+CNT collector was more than 2.5 times higher than that of the only PC collector (see Fig. 6).

4.2. Solar absorptivity, α_2 , of the PC+CNT layer and the heat transfer rate estimation

By using the measured temperatures, the optical properties of the PC+CNT layer could be estimated. The measured ambient (T_a), water inlet (T_{in}), and water outlet (T_{out}) temperatures of the first CNT collector are listed in Table 5. The total amount of heat transferred to the water (4th column in Table 5) can be calculated with the measured water temperature variations considering conservation of energy;

The total amount of heat transferred to the water should be identical with the net heat gain by the absorbing layers under the assumption of no heat loss between the absorbing layers and water. The total (net) heat gain of the absorbing layers can be obtained by the subtraction of the heat losses from the upper absorbing layer by radiation and natural convection from the solar energy absorbed in both the upper and lower layers of the

water channel (eq. 5). The total heat transfer rate is a function of the temperatures of the layers, the optical properties (e.g. solar absorptivity, α , and transmissivity, τ , of the layers), and the geometric parameters (e.g. the height of the air gap, H_1). By using the measured temperatures and the known dimensions of the collector, some of the optical properties of the absorbing layer can be estimated. The averaged value of the measured surface temperatures on the absorbing layer (T_2 in Table 5) is also computed for this estimation. The primary interest must be on the absorptivity of the solar absorption layer. Under the assumptions of the base properties (see Table 1), the solar absorptivity (α_2) of the PC+CNT layer was calculated by using the obtained total heat flux and the averaged surface temperature (T_2) and listed in Table 5. Finally, the solar radiation absorptivity of the PC+CNT layer was determined to be around 0.33 which is more than three times of the polycarbonate absorptivity (typically, 0.09). It is consistent with the measured efficiencies of two solar collectors in the first test as shown in Fig. 6. Therefore, the inclusion of CNT significantly improved the solar absorption of the polycarbonate as expected.

Tab. 5: Measured temperatures and heat transfer of the first PC+CNT collector

T_a (°C)	T_{in} (°C)	T_{out} (°C)	q_{total} (W/m ²) to water	T_2 (°C)	α_2	q_{total} (W/m ²) for $\alpha_2 = 0.4$	Heat loss
19.44	21.64	25.08	305.38	30.85	0.358	347	13%
20.73	25.57	28.23	236.14	34.91	0.308	328	28%
20.61	29.33	31.97	234.36	38.94	0.328	306	24%
21.13	33.34	35.63	203.29				

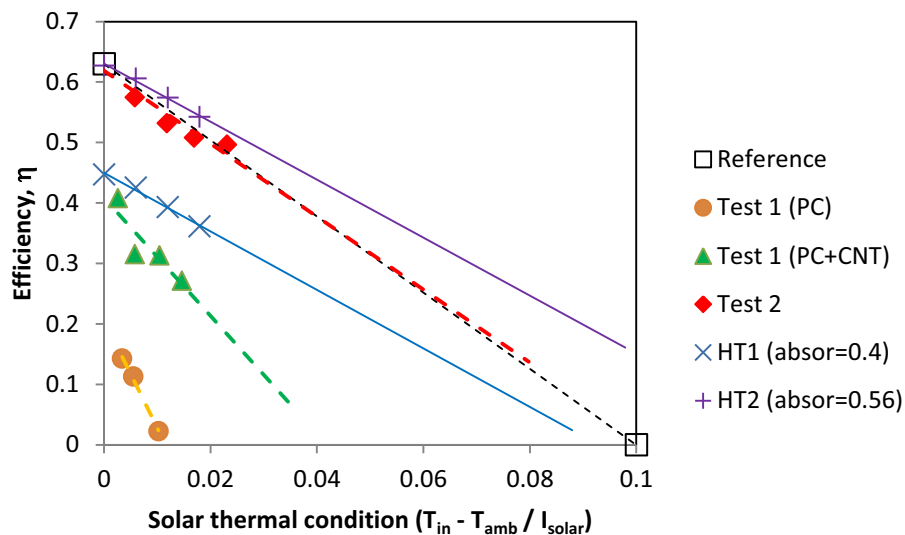


Fig. 6: The tested and estimated efficiencies of the solar collectors

Due to the entrapped air and relatively small size of panel, the heat absorbed into the PC+CNT layer was not able to be fully transferred to the water. Taking account of this detrimental effect, the actual solar absorptivity of the PC+CNT layer would be higher than 0.33. The maximum amount of heat gain with the assumed solar radiation absorptivity of 0.4 was estimated (without heat loss) and given in Table 5. By comparing between the actually obtained total heat flux and the ideal estimation with $\alpha_2 = 0.4$, the estimation of the heat losses due to the entrapped air, leakages and edge effects would be more than 25% (Table 5).

Thereafter, the second test of the improved prototype (1500 × 500 mm) was conducted at a series of increasing inlet temperatures while measuring the energy absorption of the collector. The result showed the performance of the second PC+CNT collector was significantly higher than that of the collectors in the first test (Fig. 6). The developed PC+CNT solar collector performed equivalently to the reference of the conventional glazed flat plate solar collector with moderately selective black paint absorber. Eventually, the polymer-carbon nanotubes based solar collector which has a comparable efficiency with a conventional solar collector has been successfully developed.

4.3. Design of production model

The fabricated prototypes units had limitations in both structural strength and aesthetics due to the need to use readily available polymer sheeting and sections in the construction. However, the investment in tooling associated with a volume production model allows more freedom in the design to achieve a more aesthetic product, reduced joints, simplified manufacture and a more rigid assembly. When polycarbonate material is exposed to water at elevated temperature (more than 60 °C) for a sustained period of time, it can experience degradation of mechanical properties due to hydrolysis. Due to the risk of hydrolysis of polycarbonate occurring in this particular application, other polymer materials were considered for the construction of the water channel section in the production model. The two most promising alternative materials were polypropylene and polyamide, which can be glass filled to produce a stronger composite material. The use of glass filled polyamide in contact with hot water under pressure is common in the automotive industry.

The basic design concept is to make a polymer solar collector of acceptable efficiency with as few parts as possible, which is serviceably light and easy to install. Importantly, the production unit should minimize the number of joints in order to reduce risks of leak and minimize production costs. Finally, the overall assembly requires two special extruded components; the water cavity and the outer insulation cover. It requires one special injection moulded component - the end cap, and one formed component – the pipe cover. Other components are standard sheets or proprietary components that can be sourced from existing suppliers. The design therefore minimises the investment in tooling, achieves a simple assembly process and has only two joints in each panel that need to be of a water tight standard. The estimated cost of the production model is around £80 per square meter based on current market prices of materials and fabrication. It is two times less than that of the conventional flat plate solar collectors, £150 – £230 per square meter.

5. Conclusion

The polymer-carbon nanotubes based solar collector was designed as a multi-layer structure with considering the cost-effective manufacturing. Through the mathematical heat transfer analysis, the performance and characteristics of the solar collector have been estimated. The prototypes of the proposed system were built and tested at a state-of-the-art solar simulator facility to evaluate the actual performance of the developed solar collector. The inclusion of CNT improved around three times the solar absorption of the polycarbonate. The efficiency of the second (improved) prototype reached equivalently the practical maximum of this type (a glazed flat plate) of solar collector. Eventually, the cost-effective polymer-CNT based solar collector, which achieved similar efficiency compared to the conventional glazed flat plate solar panel, will be able to be developed with two times less cost.

6. References

- Abtahi, A., 1993. Low-cost solar water heating: the breadbox heater made with recycled plastics, *Proceedings I.S.E.S. Solar World Conf.*, 5, 347-352.
- DECC, 2012. UK Renewable Energy Roadmap Update 2012. https://www.gov.uk/government/uploads/system/uploads/attachment_data/file/80246/11-02-13_UK_Renewable_Energy_Roadmap_Update_FINAL_DRAFT.pdf (August 2014)
- Dorfling, C., Hornung, C.H., Hallmark, B., Beaumont, R.J.J., Fovargue, H., Mackley, M.R., 2010. The experimental response and modelling of a solar heat collector fabricated from plastic microcapillary films. *Solar Energy Materials & Solar Cells*. 94, 1207-1221.
- Kudish, A. I., Evseev, E. G., Walter, G. Leukefeld, T., 2002. Simulation study of a solar collector with a selectively coated polymeric double walled absorber plate, *Energy Conversion & Management*, 43, 651-671.
- Mark, J. E., 2007. *Physical Properties of Polymers Handbook*, Springer.
- Tsiliniris, P.T., 1999. Towards making solar water heating technology feasible – the polymer double walled absorber plate. *Energy Conversion & Management*. 40, 1237-1250.
- Tripanagnostopoulos, Y., Souliotis, M., Nousia, T., 2000. Solar collectors with coloured absorbers, *Solar Energy*, 68, 343-356.
- Wijeysundera, N.E., Iqbal, M., 1991. Effect of plastic cover thickness on the top loss coefficient of FPSCs. *Solar Energy*, 2, 83-87.